

# Light unflavor vector meson spectroscopy around the mass range of 2.4 ~ 3 GeV and possible experimental evidence

Li-Ming Wang<sup>1,3,\*</sup>, Si-Qiang Luo<sup>2,3,4,†</sup> and Xiang Liu<sup>2,3,4,5,‡§</sup>

<sup>1</sup>Key Laboratory for Microstructural Material Physics of Hebei Province,  
School of Science, Yanshan University, Qinhuangdao 066004, China

<sup>2</sup>School of Physical Science and Technology, Lanzhou University, Lanzhou 730000, China

<sup>3</sup>Lanzhou Center for Theoretical Physics, Key Laboratory of Theoretical Physics of Gansu Province  
and Frontiers Science Center for Rare Isotopes, Lanzhou University, Lanzhou 730000, China

<sup>4</sup>Research Center for Hadron and CSR Physics, Lanzhou University and Institute of Modern Physics of CAS, Lanzhou 730000, China

<sup>5</sup>Joint Research Center for Physics, Lanzhou University and Qinghai Normal University, Xining 810000, China

(Dated: September 15, 2021)

In this work, we predict the spectroscopy behavior of these light unflavor vector mesons with masses at the range of 2.4 ~ 3 GeV, which are still missing in experiment. By presenting their mass spectrum and studying their two-body Okubo-Zweig-lizuka allowed decay widths, we discuss the possible experimental evidences of these discussed states combing with the present experimental data. Especially, we strongly suggest our experimental colleague to carry out the exploration of these higher states via the  $e^+e^-$  annihilation into light mesons. It is obvious that BESIII and Belle II will be potential experiment to achieve this target.

## I. INTRODUCTION

As the accepted theory depicting the strong interaction, quantum chromodynamics (QCD) is successful in the high-energy regime, where there exists asymptotic freedom phenomenon. However, in the low-energy regime, how to quantitatively describe the nonperturbative behavior of QCD which has close relation with the confinement physics remains challenge. Obviously, studying the light hadron spectroscopy may deep our understanding of this problem.

Focusing on the study of light unflavor vector meson spectroscopy, we find big progress made by experiment in the past years [1–3]. A typical example is the observation of the  $Y(2175)$  [4] and the following measurement [5–10] around the  $Y(2175)$ , which have stimulated extensive discussions of decoding the property of the  $Y(2175)$  [11–16]. Among these discussions, whether or not the  $Y(2175)$  can be categorized into  $\phi$  meson family becomes a long-stranding issue [11, 17, 18]. In fact, the light unflavor vector mesons also include these states in the  $\rho$  and  $\omega$  meson families. With the accumulation of data with unprecedented statistical accuracy, the  $\rho$  and  $\omega$  state around 2 GeV appeared in front of people [19–27]. By the join effort from both theoretical and experimentalist, our knowledge of light unflavor vector meson spectroscopy below 2.2 GeV has been promoted, which is the situation of the study of unflavor vector meson spectroscopy. But, it is not the whole aspect of light unflavor vector meson spectroscopy.

The experiments have released the data of  $e^+e^-$  annihilation into light mesons [28–31], where the collision energy reaches up to ~ 3 GeV. When checking these data, we find possible enhancement structures existing in the corresponding invariant mass spectra with mass range from 2.4 GeV to 3 GeV. For

example, in the  $e^+e^- \rightarrow \omega\pi^+\pi^-\pi^0$  process [28], several enhancement structures existing in the energy range of 2.4 GeV are obvious. However, in the process of  $e^+e^- \rightarrow \pi^+\pi^-\pi^0$ , we cannot find conspicuous enhancement structure [29]. Thus, we still need more precise data. In the following, we can find many narrow structures above 2.4 MeV in the process of  $e^+e^- \rightarrow K_2^{*0}(1430)K^-\pi^+$  reported by the BaBar Collaboration [30]. The cross section of  $e^+e^- \rightarrow \phi f_2'(1525)$  was also measured by the BaBar Collaboration. Here, there exist possible enhancement clusters around 2.7 GeV and a clear  $J/\psi$  signal [30]. And then, the Belle Collaboration studied the process of  $e^+e^- \rightarrow \phi\pi^+\pi^-$  and  $e^+e^- \rightarrow \phi f_0(980)$  [31], where the event accumulation around 2.4 GeV and 2.6 GeV can be found. We conjecture that these enhancement structures with low significance can be due to these unknown light unflavor vector mesons.

At present, our knowledge of higher states of light unflavor vector meson family, which have the masses above 2.4 GeV, is obviously absent. This research status makes us to reinforce investigation of these higher states of light unflavor vector meson family, which becomes a central task of this work.

In this work, we apply the modified Godfrey-Isgur model [32] to present the masses distribution of the discussed higher states of light unflavor vector meson family, where their spatial wave functions can be get numerically, which can be as the input of the following calculation of their two-body Okubo-Zweig-lizuka (OZI) allowed decays. For performing the realistic estimate of these OZI allowed decays, the quark pair creation (QPC) model is adopted here [33–35], which was applied to study the strong decay of different kinds of hadron [17, 36–44]. We hope that the focused light unflavor vector meson behavior can be obtained, which is helpful to further experimental exploration.

As emphasized in Ref. [45], the BESIII experiment at the BEPCII electron-positron collider is still an ideal platform to hunt for light hadrons. We have reason to believe that the present work can attract the BESIII interest of studying this topic in experiment. In addition, the running Belle II with Initial State Radiation (ISR) method will be a potential exper-

\*Corresponding author

\*Electronic address: [lmwang@ysu.edu.cn](mailto:lmwang@ysu.edu.cn)

†Electronic address: [luosq15@lzu.edu.cn](mailto:luosq15@lzu.edu.cn)

§Electronic address: [xiangliu@lzu.edu.cn](mailto:xiangliu@lzu.edu.cn)

iment to finding these discussed light unflavor vector mesons.

This paper is organized as follows. After the Introduction in Sec. I, we present the spectroscopy behavior by the MGI model and the QPC model, where the mass spectrum and two-body OZI allowed strong decays of these discussed higher states of light unflavor vector meson are given in Sec. II. Finally, the paper ends with a short summary in Sec. III.

## II. SPECTROSCOPY BEHAVIOR

For presenting some aspect of of light unflavor vector meson spectroscopy, we adopt phenomenological models. In this work, the modified Godfrey-Isgur (MGI) model is applied to give the mass spectrum [32], where the obtained spatial wave functions of these involved higher light unflavor mesons are as input when furthering getting the two-body OZI allowed strong decay of them via the QPC model. In Fig. 1, we show the procedure of how to obtain the whole aspect of these higher light unflavor vector meson spectroscopy.

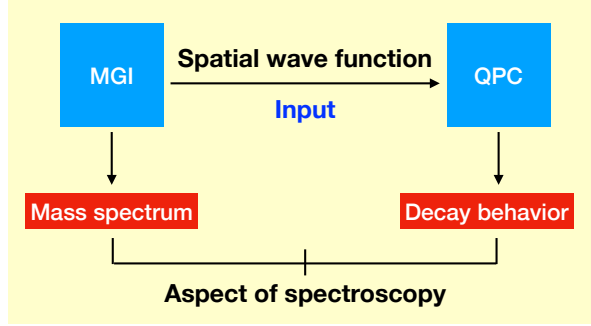


FIG. 1: The procedure of presenting the aspect of light unflavor vector meson spectroscopy.

### A. Mass spectrum

The Hamiltonian depicting the interaction between quark and antiquark in the MGI model is

$$\tilde{H} = \sqrt{m_1^2 + \mathbf{p}^2} + \sqrt{m_2^2 + \mathbf{p}^2} + \tilde{V}_{\text{eff}}(\mathbf{p}, \mathbf{r}), \quad (1)$$

where  $m_1$  and  $m_2$  denote the mass of quark and antiquark, respectively. The effective potential of the  $q\bar{q}$  interaction has the form [46]

$$\tilde{V}_{\text{eff}}(\mathbf{p}, \mathbf{r}) = \tilde{H}^{\text{conf}} + \tilde{H}^{\text{so}} + \tilde{H}^{\text{hyp}}, \quad (2)$$

which contains a short  $\gamma^\mu \otimes \gamma_\mu$  one-gluon-exchange interaction and a  $1 \otimes 1$  linear confining interaction. Additionally, the effective potential can be written as

$$V_{\text{eff}}(\mathbf{p}, \mathbf{r}) = H^{\text{conf}} + H^{\text{so}} + H^{\text{hyp}} \quad (3)$$

with

$$H^{\text{conf}} = \left[ -\frac{3}{4}(c + br) + \frac{\alpha(r)}{r} \right] (\mathbf{F}_1 \cdot \mathbf{F}_2) \quad (4)$$

$$= S(r) + G(r),$$

where  $H^{\text{conf}}$  contains the spin-independent linear confinement  $S(r)$  and Coulomb-type interaction  $G(r)$ . In the MGI model, the screen effect [32] is introduced, where we should make a replacement in Eq. (4) as

$$br \rightarrow V^{\text{scr}}(r) = \frac{b(1 - e^{-\mu r})}{\mu}. \quad (5)$$

And

$$H^{\text{hyp}} = -\frac{\alpha_s(r)}{m_1 m_2} \left[ \frac{8\pi}{3} \mathbf{S}_1 \cdot \mathbf{S}_2 \delta^3(\mathbf{r}) \right. \quad (6)$$

$$\left. + \frac{1}{r^3} \left( \frac{3\mathbf{S}_1 \cdot \mathbf{r} \mathbf{S}_2 \cdot \mathbf{r}}{r^2} - \mathbf{S}_1 \cdot \mathbf{S}_2 \right) \right] (\mathbf{F}_1 \cdot \mathbf{F}_2)$$

is the color hyperfine interaction. And then,

$$H^{\text{so}} = H^{\text{so}(\text{cm})} + H^{\text{so}(\text{tp})} \quad (7)$$

is the spin-orbit interaction with

$$H^{\text{so}(\text{cm})} = -\frac{\alpha_s(r)}{r^3} \left( \frac{1}{m_1} + \frac{1}{m_2} \right) \left( \frac{\mathbf{S}_1}{m_1} + \frac{\mathbf{S}_2}{m_2} \right) \cdot \mathbf{L} (\mathbf{F}_1 \cdot \mathbf{F}_2) \quad (8)$$

and

$$H^{\text{so}(\text{tp})} = -\frac{1}{2r} \frac{\partial H^{\text{conf}}}{\partial r} \left( \frac{\mathbf{S}_1}{m_1^2} + \frac{\mathbf{S}_2}{m_2^2} \right) \cdot \mathbf{L}. \quad (9)$$

In the above formula,  $\mathbf{S}_1$  and  $\mathbf{S}_2$  denote the spin of quark and antiquark, respectively.  $\mathbf{L}$  indicates the orbital momentum between two quarks while  $\mathbf{F}$  is related to the Gell-Mann matrices in color space. In addition, we take  $\langle \mathbf{F}_1 \cdot \mathbf{F}_2 \rangle = -4/3$  for meson system. More details of the MGI model can be found in Ref. [32].

TABLE I: The value of these parameters involving in the MGI model.

| Parameter               | Value  | Parameter               | Value  |
|-------------------------|--------|-------------------------|--------|
| $m_u$ (GeV)             | 0.22   | $m_d$ (GeV)             | 0.22   |
| $m_s$ (GeV)             | 0.424  | $b$ (GeV <sup>2</sup> ) | 0.229  |
| $\epsilon_c$            | -0.164 | $\epsilon_{\text{sos}}$ | 0.9728 |
| $\sigma_0$ (GeV)        | 1.8    | $s$ (GeV)               | 3.88   |
| $\mu$ (GeV)             | 0.081  | $c$ (GeV)               | -0.30  |
| $\epsilon_{\text{sov}}$ | 0.262  | $\epsilon_t$            | 1.993  |

The values of all parameters used in the MGI model are collected in Table I. With these preparation, we further present the mass spectrum of light unflavor vector meson in Fig. 2. Here, besides reproducing the masses of these low lying states, the masses of higher states are also obtained. Our calculated result explicitly shows that there exists accumulation

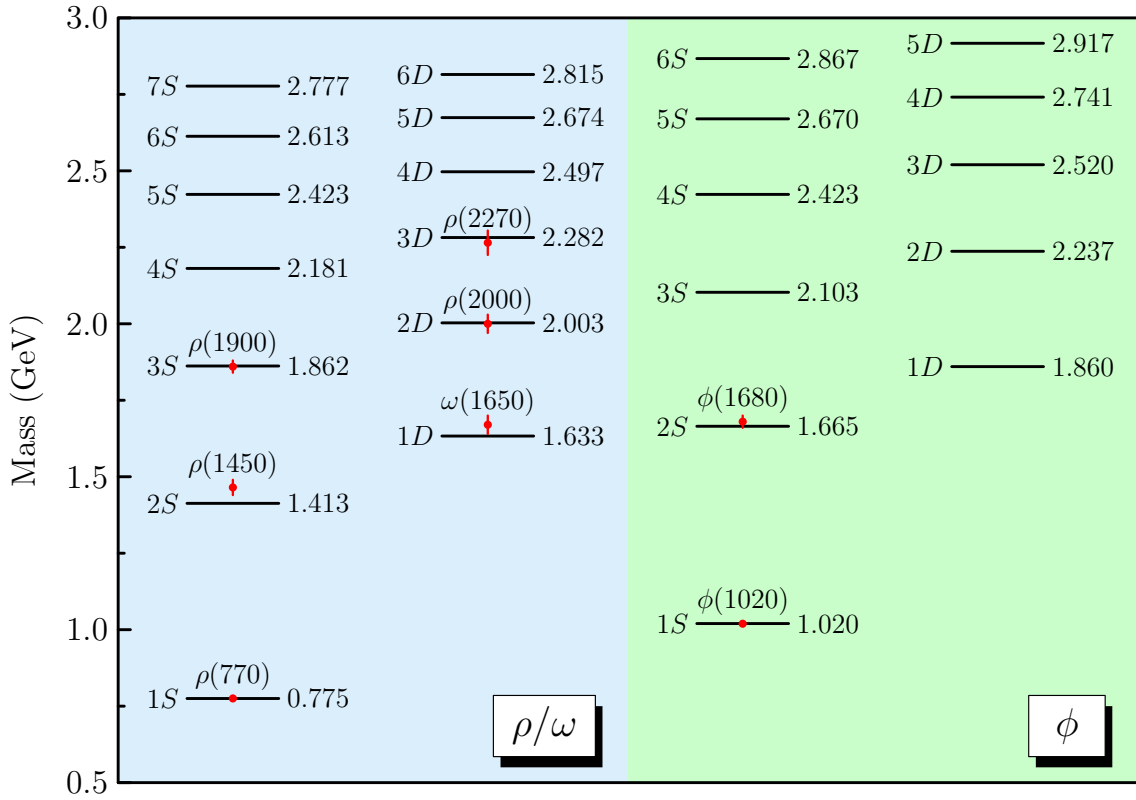


FIG. 2: The comparison of calculated result calculated in this work and the experimental data of mass of higher  $\rho$ ,  $\omega$  and  $\phi$  states. Here, the red dots denote the experimental data from Refs. [22, 28, 47, 48].

of these 5S, 6S, and 7S states of  $\rho$ ,  $\omega$  and  $\phi$  mesons in the mass range from 2.4 GeV to 3 GeV.

When having the theoretical results of masses of these higher states of light unflavor vector mesons, we can make comparison of our result with the experimental data as shown in Fig. 3. Firstly, focusing on the data of  $e^+e^- \rightarrow \omega\pi^+\pi^-\pi^0$  [28] which has close relation with higher  $\rho$  mesons due to the  $G$ -parity conservation, we find that the invariant mass distribution shows obvious enhancement structures like the event accumulation around 2.65 GeV. This broad structure overlaps with the predicted  $\rho(6S)$  and  $\rho(5D)$  states. There exists a jump point around 2.76 GeV, which may corresponds to  $\rho(7S)$ . And then, an unnotable fluctuation around 2.81 GeV just locates at the position of  $\rho(6D)$ . Additionally, a bump structure around 2.4 GeV should have relation with  $\rho(5S)$ , while around the  $\rho(4D)$  state we can also find an obvious jump point.

The data of  $e^+e^- \rightarrow \pi^+\pi^-\pi^0$  [29] is an ideal process to identify  $\omega$  states. Although we mark these predicted  $\omega$  states in the corresponding cross section data, we cannot identify the obvious bump structure corresponding to these states since the precision of the measured data is not enough. Thus, we have to wait for further precise measurement of the cross section of  $e^+e^- \rightarrow \pi^+\pi^-\pi^0$ .

In the following, we check four measured processes  $e^+e^- \rightarrow K_2^{*0}(1430)K^-\pi^+$  [30],  $e^+e^- \rightarrow \phi\pi^+\pi^-$  [31],  $e^+e^- \rightarrow \phi f_0(980)$  [31], and  $e^+e^- \rightarrow \phi f_2(1525)$  [30]. For  $e^+e^- \rightarrow K_2^{*0}(1430)K^-\pi^+$ , there exist abundant event clusters. Since

these predicted higher  $\rho$ ,  $\omega$  and  $\phi$  states can decay into open-strange meson pair, it is difficult to distinguish  $\rho$ ,  $\omega$  and  $\phi$  states via the  $e^+e^- \rightarrow K_2^{*0}(1430)K^-\pi^+$  channel. Further data analysis of  $e^+e^- \rightarrow K_2^{*0}(1430)K^-\pi^+$  is an interesting research issue similar to the way adopted in Refs. [12, 49].

Different from  $e^+e^- \rightarrow K_2^{*0}(1430)K^-\pi^+$ ,  $e^+e^- \rightarrow \phi f_0(980)$  can be ideal process to identify these higher  $\phi$  states. Two obvious structures around 2.4 GeV and 2.7 GeV may correspond to  $\phi(4S)$  and  $\phi(5S)$ , respectively. Of course, we may also find an event accumulation around 2.5 GeV corresponding to  $\phi(3D)$ . For  $e^+e^- \rightarrow \phi\pi^+\pi^-$ , the structure at 2.41 GeV and the enhancement around 2.7 GeV may have relation to the  $\phi(4S)$ ,  $\phi(5S)/\phi(4D)$ . For  $e^+e^- \rightarrow \phi\pi^+\pi^-$ , the broad structure around 2.65 GeV contains the information of the predicted  $\phi(5S)/\phi(4D)$ . Generally speaking, we expect more precise data, which can be applied to identify these discussed higher light unflavor vector mesons.

Although we discuss the possible evidences of the prediction of higher light unflavor vector mesons focused by us, their mass spectrum behaviors only provide one aspect of spectroscopy. In the following section, we pay more attention to their two-body OZI allowed strong decays, which can give important hint of experimental search for them. Here, we need to emphasize that the numerical forms of the spatial wave function of these discussed light unflavor mesons can be obtained, which are as the input of the following discussion of their decay behavior.

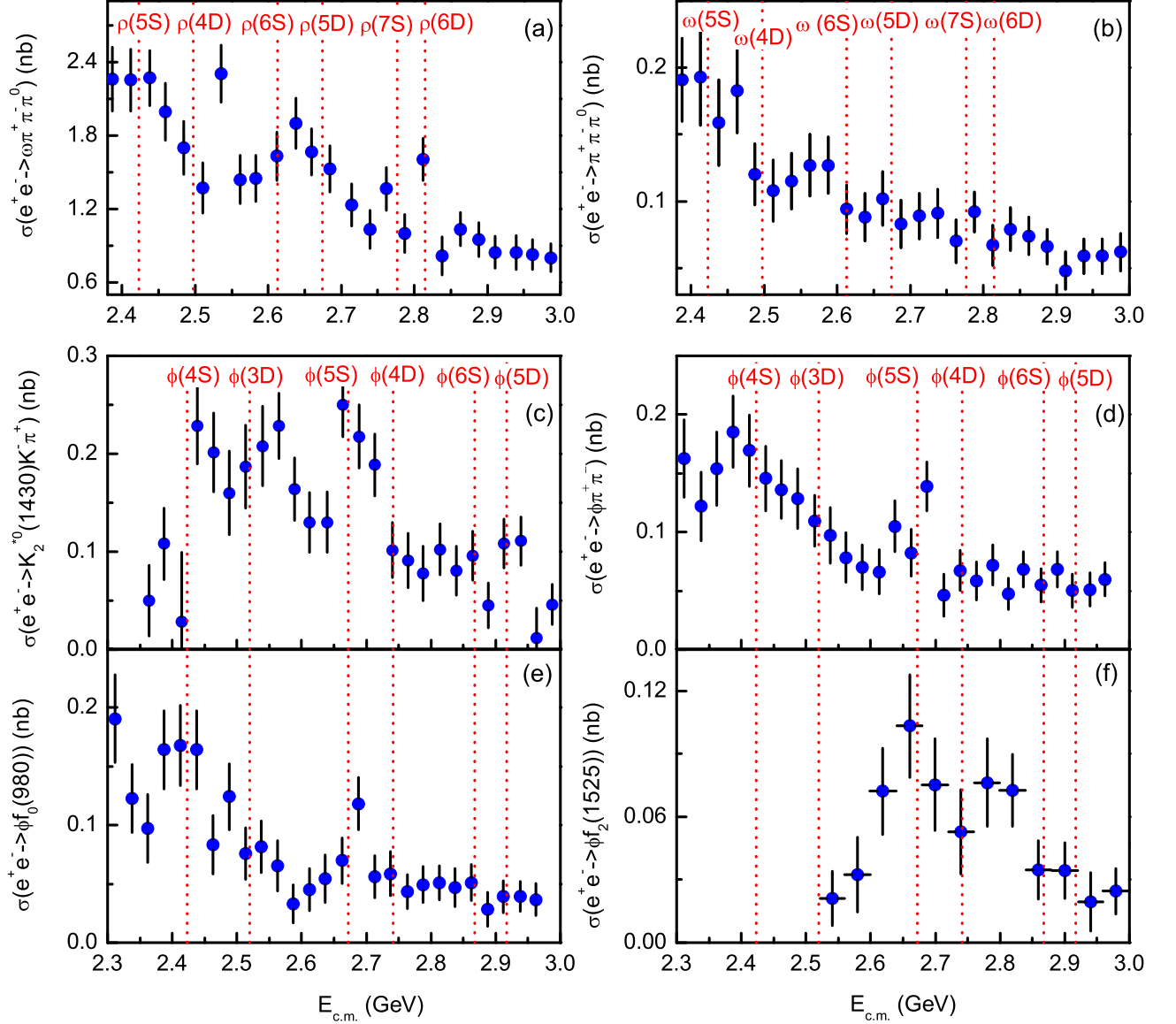


FIG. 3: A comparison of theoretical masses of these discussed light vector  $\rho$ ,  $\omega$  and  $\phi$  mesons and the experimental data of  $e^+e^- \rightarrow \omega\pi^+\pi^-\pi^0$  [28],  $e^+e^- \rightarrow \pi^+\pi^-\pi^0$  [29],  $e^+e^- \rightarrow K_2^{*0}(1430)K^-\pi^+$  [30],  $e^+e^- \rightarrow \phi\pi^+\pi^-$  [30],  $e^+e^- \rightarrow \phi f_0(980)$  [30], and  $e^+e^- \rightarrow \phi f_2(1525)$  [30].

### B. Two-body OZI allowed strong decay

For calculating the two-body OZI allowed strong decay of these discussed higher unflavor vector meson states, we apply the QPC model, which is an effective approach to quantitatively estimate such physical quantity [33–35].

In the QPC model, when a meson decay occurs, a quark-antiquark pair is created from vacuum with the quantum number  $J^{PC} = 1^{++}$ , and combines with the corresponding antiquark and quark in the initial meson to produce two final mesons. The general expression of the mock state wave func-

tion involving in the process  $A \rightarrow B + C$  is defined by [35]

$$\begin{aligned}
 & \left| A \left( n_A^{2S_A+1} L_{AJ_A M_{J_A}} \right) (P_A) \right\rangle \\
 & \equiv \sqrt{2E_A} \sum_{M_{L_A}, M_{S_A}} \langle L_A M_{L_A} S_A M_{S_A} | J_A M_{J_A} \rangle \\
 & \times \int d^3 \mathbf{p}_A \psi_{n_A L_A M_{L_A}}(\mathbf{p}_A) \chi_{S_A M_{S_A}}^{12} \phi_A^{12} \omega_A^{12} \\
 & \times \left| q_1 \left( \frac{m_1}{m_1 + m_2} \mathbf{P}_A + \mathbf{p}_A \right) \bar{q}_2 \left( \frac{m_2}{m_1 + m_2} \mathbf{P}_A + \mathbf{p}_A \right) \right\rangle,
 \end{aligned}$$

where  $m_1$  and  $m_2$  are masses of quark  $q_1$  and antiquark  $\bar{q}_2$  respectively.  $n_A$  is the radical quantum number of meson  $A$  with the  $q_1 \bar{q}_2$  quark component.  $S_A$  and  $L_A$  denote spin and

relative orbital angular momentum between  $q_1$  and  $\bar{q}_2$ , respectively.  $\mathbf{J}_A = \mathbf{S}_A + \mathbf{L}_A$  is the total spin.  $\mathbf{P}_A = \mathbf{p}_1 + \mathbf{p}_2$  and  $E_A$  are CM momentum and total energy of meson  $A$ , respectively.  $\mathbf{p}_A = \frac{m_1\mathbf{p}_1 - m_2\mathbf{p}_2}{m_1 + m_2}$  is relative momentum of  $q_1\bar{q}_2$  pair, where  $\mathbf{p}_1$  and  $\mathbf{p}_2$  is momentum of  $q_1$  and  $\bar{q}_2$ , respectively.  $\chi_{S_A M_{S_A}}^{12}$ ,  $\phi_A^{12}$  and  $\omega_A^{12}$  are the spin, flavor and color wave function, respectively.  $\psi_{n_A L_A M_{L_A}}(\mathbf{p}_A)$  represents space wave function of meson  $A$ .

The total decay width in the centre-of-mass (CM) frame is given by

$$\Gamma = \frac{\pi}{4} \frac{|\mathbf{P}|}{M_A^2} \sum_{LS} |M^{LS}|^2. \quad (10)$$

Here,  $\mathbf{P}$  is the momentum outgoing meson (meson  $B$  or meson  $C$ ).  $M_A$  is the mass of meson  $A$ .  $\mathbf{L}$  and  $\mathbf{S}$  denote the relative orbital angular and total spin momentum between meson  $B$  and  $C$ , respectively.  $M^{LS}$  denotes the partial wave amplitude and is related to the helicity amplitude  $M^{M_{J_A} M_{J_B} M_{J_C}}$  according to Jacob-Wick formula [50]. In the CM frame, the specific form of  $M^{M_{J_A} M_{J_B} M_{J_C}}$  can be written as

$$\begin{aligned} & M^{M_{J_A} M_{J_B} M_{J_C}}(\mathbf{P}) \\ &= \gamma \sqrt{8E_A E_B E_C} \sum_{M_{L_A}, M_{S_A}, M_{L_B}, M_{S_B}, M_{L_C}, M_{S_C}} \langle L_A M_{L_A} S_A M_{S_A} | J_A M_{J_A} \rangle \\ & \times \langle L_B M_{L_B} S_B M_{S_B} | J_B M_{J_B} \rangle \langle L_C M_{L_C} S_C M_{S_C} | J_C M_{J_C} \rangle \\ & \times \langle 1m1 - m | 00 \rangle \langle \chi_{S_B M_{S_B}}^{14} \chi_{S_C M_{S_C}}^{32} \chi_{S_A M_{S_A}}^{12} \chi_{1-m}^{34} \rangle \\ & \times \left[ \langle \phi_B^{14} \phi_C^{32} | \phi_A^{12} \phi_0^{34} \rangle I(\mathbf{P}, m_2, m_1, m_3) \right. \\ & \left. + (-1)^{1+S_A+S_B+S_C} \langle \phi_B^{32} \phi_C^{14} | \phi_A^{12} \phi_0^{34} \rangle I(-\mathbf{P}, m_2, m_1, m_3) \right], \end{aligned}$$

where  $\gamma$  as the strength of quark-antiquark pair created from vacuum is fixed to be 6.57 [51].  $\phi_0$  denotes the flavor wave function of this quark-antiquark pair.  $I(\mathbf{P}, m_2, m_1, m_3)$  is the momentum space integral

$$\begin{aligned} I(\mathbf{P}, m_2, m_1, m_3) &= \int d^3 \psi_{n_B L_B M_{L_B}}^* \left( \frac{m_3}{m_1 + m_3} \mathbf{P} + \mathbf{p} \right) \\ & \times \psi_{n_C L_C M_{L_C}}^* \left( \frac{m_3}{m_2 + m_3} \mathbf{P} + \mathbf{p} \right) \\ & \times \psi_{n_A L_A M_{L_A}}(\mathbf{P} + \mathbf{p}) \mathcal{Y}_1^m(\mathbf{p}), \end{aligned} \quad (11)$$

where  $\mathcal{Y}_1^m(\mathbf{p})$  is a solid harmonic that gives the momentum space distribution of created quark-antiquark pair.

With the above preparation, we can estimate the strong decay behavior of these discussed vector mesons, which is main task of the following subsections.

### 1. $\rho$ states

As shown in Fig. 2, there are six  $\rho$  states ( $\rho(5S)$ ,  $\rho(6S)$ ,  $\rho(7S)$ ,  $\rho(4D)$ ,  $\rho(5D)$ ,  $\rho(6D)$ ) existing in the mass range of 2.4 ~ 3 GeV.

The obtained total and main partial decay widths of  $\rho(5S)$  are shown in Fig. 4, which show that  $\pi a_2(1700)$  is the dominant decay channel and the total width of  $\rho(5S)$  can reach up to 81.85 MeV. In Fig. 4, we also list their several typical decay modes like  $\pi\pi$  and  $\pi\omega$  easily accessible at experiment. However, the branching ratios of these typical decays are not obvious. Of course, the  $\rho(5S)$  state can also decay into open-strange meson pair. However, our result shows that their contribution to the total width is not significant. For example,  $\rho(5S) \rightarrow KK_1(1270)$  and  $K^*K_1(1270)$ , have branching ratios of 0.43% and 0.41%, respectively. Thus, in this work, we do not collect the decay channels relevant to the open-strange meson pair in Fig. 4.

The predicted decay behavior of  $\rho(6S)$  is given in Fig. 4. Similar to the  $\rho(5S)$  state, its dominant decay channel is also  $\pi a_2(1700)$ , while the  $\rho\rho(1450)$ ,  $\pi\pi_2(1880)$ ,  $\pi\pi(1800)$  and  $\pi\pi(1300)$  modes have sizable contributions to the total decay width, which is predicted to be around 57.25 MeV. Additionally, the particle widths of  $KK_1(1270)$  and  $K^*K_1(1270)$  are 0.18 MeV and 0.16 MeV, respectively, which are not listed in Fig. 4.

The calculation results for the  $\rho(7S)$  are presented in Fig. 4, where  $\rho\rho(1450)$  and  $\pi\pi_2(1880)$  are its dominant decay modes. In addition, the contribution of the  $\pi\pi(1800)$ ,  $\pi a_2(1700)$ ,  $\pi\pi(1300)$  and  $\rho\rho$  decay modes to total width cannot ignored. As the typical channels,  $\pi\pi$  and  $\pi\omega$  have the branching ratios of 1.09% and 0.10%, respectively.

Accompanying with these three  $S$ -wave states, three corresponding  $D$ -wave states exist in the same mass range. In Fig. 4, the two-body OZI allowed strong decay behavior of  $\rho(4D)$ ,  $\rho(5D)$ ,  $\rho(6D)$  are given by presenting the total decay width and the branching ratios of their partial decays. The total decay widths of  $\rho(4D)$ ,  $\rho(5D)$ ,  $\rho(6D)$  are 92.33 MeV, 55.69 MeV, and 32.96 MeV, respectively, where their main decay modes are  $\pi\pi_2(1880)$ ,  $\pi\pi(1300)$  and  $\pi\pi(1800)$ . Since these three  $D$ -wave  $\rho$  states have sizable  $\pi\pi$  decay rate, the  $e^+e^- \rightarrow \pi\pi$  process can be as the ideal channel to identify these  $D$ -wave  $\rho$  states, which should stimulate experimentalist's interest in measuring the cross section of  $e^+e^- \rightarrow \pi\pi$  with energy of collision up to 3 GeV.

### 2. $\omega$ states

In the following, we check the two-body OZI allowed strong decay of six higher  $\omega$  mesonic states, which include  $\omega(5S)$ ,  $\omega(6S)$ ,  $\omega(7S)$ ,  $\omega(4D)$ ,  $\omega(5D)$  and  $\omega(6D)$ , where their total decay widths and partial decay widths estimated by the QPC model are shown in Fig. 4.

The total widths of  $\omega(5S)$  and  $\omega(6S)$ , which are contributed by the main decay channels like  $\rho a_0(1450)$ ,  $\pi\rho(1450)$ ,  $\rho a_1(1260)$  and  $\rho a_2(1320)$ , are 69.98 MeV and 45.10 MeV, respectively. It is worth noting that the typical mode  $\pi\rho$  has sizable contribution to the total width. Thus,  $e^+e^-$  annihilation into  $\pi\rho$  is a perfect process to experimentally search for these  $\omega$  states. Similar to the situation of the discussed  $\rho$  states,  $\omega(5S)$  and  $\omega(6S)$  decaying into open-strange meson pair are not significant.

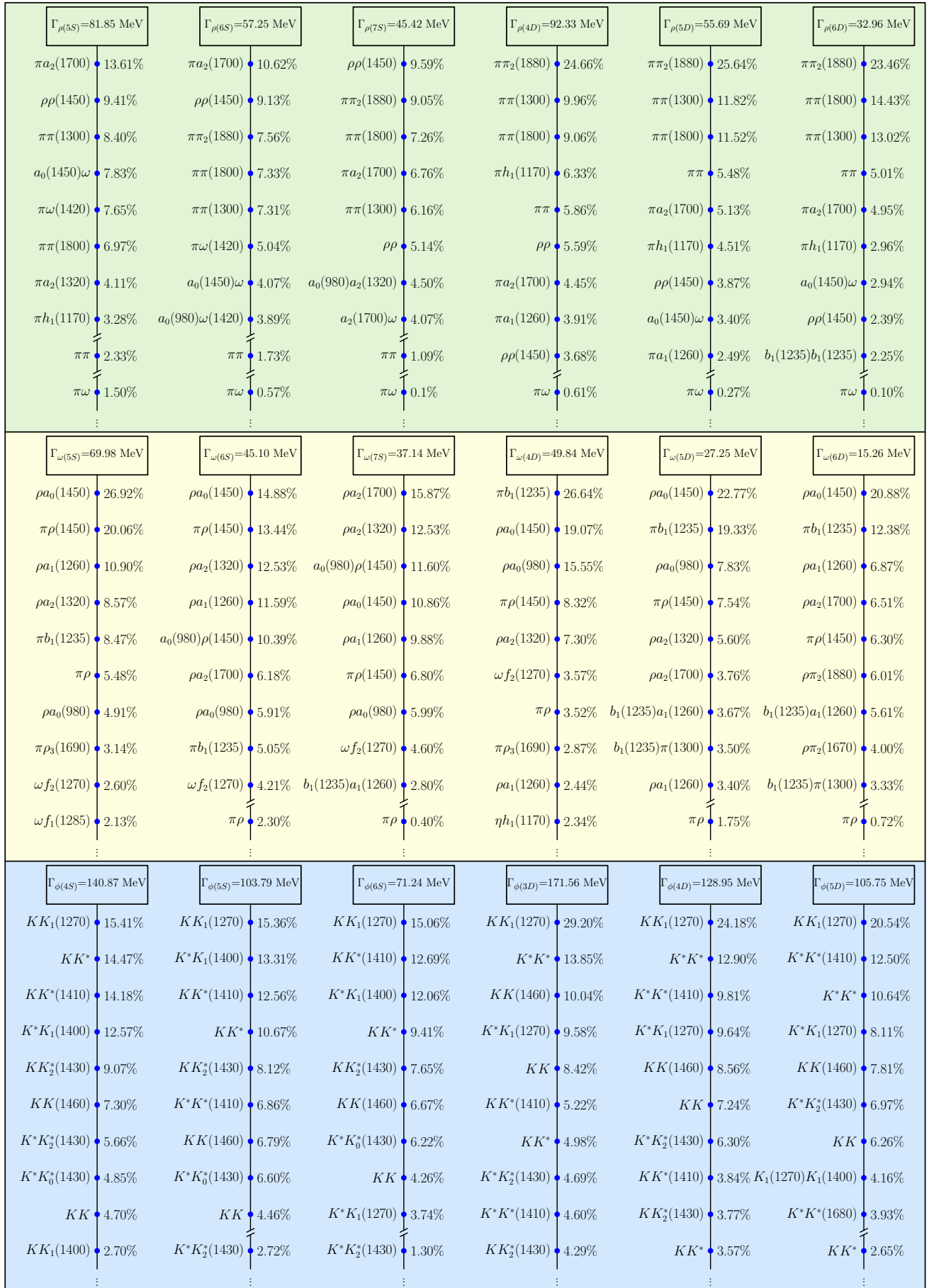


FIG. 4: The two-body strong decay behaviors of these discussed light vector mesons with the mass range from 2.4 GeV to 3 GeV. Here, we show their branching ratio of main channels and the total decay width.

The decay properties of  $\omega(7S)$  we predicted are presented in Fig. 4, where its dominant decay mode is the  $\rho a_2(1700)$  channel. Other main decay modes of  $\omega(7S)$  include  $\rho a_2(1320)$ ,  $a_0(980)\rho(1450)$ ,  $\rho a_0(1450)$ , and  $\rho a_1(1260)$ . These partial decay widths of  $\omega(7S)$  into open-strange meson pair are tiny in our calculation, which are not shown here.

Additionally, we also study three  $D$ -wave  $\omega$  states existing in the mass range  $2.4 \sim 3$  GeV. The estimated total decay width and branching ratios of partial decay of  $\omega(4D)$ ,  $\omega(5D)$  and  $\omega(6D)$  are listed in Fig. 4, where the obtained total width of  $\omega(4D)$ ,  $\omega(5D)$  and  $\omega(6D)$  are 49.84 MeV, 27.25 MeV and 15.26 MeV, respectively. These  $D$ -wave  $\omega$  states mainly decay into  $\pi b_1(1235)$  and  $\rho a_0(1450)$ . Other decay channels like  $\pi\rho(1450)$  and  $\rho a_0(980)$  also have a non-negligible effect on their total decay widths. Additionally,  $\omega(4D)$  and  $\omega(5D)$  all have sizable  $\pi\rho$  decay rate, which is more significant than  $\omega(6D)$ .

### 3. $\phi$ states

In this subsection, we discuss two-body strong decays of  $\phi(4S)$ ,  $\phi(5S)$ ,  $\phi(6S)$ ,  $\phi(3D)$ ,  $\phi(4D)$  and  $\phi(5D)$ , which are also listed in Fig. 4.

From Fig. 4, we can notice that the main decay channels of  $\phi(4S)$ ,  $\phi(5S)$  and  $\phi(6S)$  are  $KK_1(1270)$ ,  $KK^*$ ,  $KK^*(1410)$  and  $K^*K_1(1400)$ , where the total decay widths of them are 140.87 MeV, 102.28 MeV and 71.24 MeV, respectively. Due to the sizable contribution of the channel  $KK^*$  to the total decay widths of these discussed  $\phi$  states, exploring  $S$ -wave  $\phi$  mesonic states via the  $e^+e^- \rightarrow KK^*$  process is suggested.

In the same mass range, there are three  $D$ -wave  $\phi$  mesons. In this work, we also estimate their decay behaviors.  $\phi(3D)$  has the total width of 171.56 MeV, where the branching ratio of its  $KK_1(1270)$  decay channel is 29.20%, which is the main decay channel. Other modes including  $K^*K^*$ ,  $KK(1460)$ ,  $K^*K_1(1270)$  and  $KK$  are also significant. The predicted total width of  $\phi(4D)$  is 128.95 MeV. The channels of  $KK_1(1270)$ ,  $K^*K^*$ ,  $K^*K^*(1410)$  and  $K^*K_1(1270)$  have the branching ratios of 24.18%, 12.90%, 9.81% and 9.46%, respectively. And then, the obtained total decay width of  $\phi(5D)$  is 95.12 MeV in this work. The results presented in Fig. 4 further indicate that the branching ratio of the  $\phi(5D)$  decays into  $KK_1(1270)$ ,  $K^*K^*(1410)$ ,  $K^*K^*$  and  $K^*K_1(1270)$  can reach up to 20.54%, 12.50%, 10.64% and 8.11%, respectively.

Through the theoretical calculation given in this work, we find that the decay mode  $K^*K_2^*(1430)$  of six  $\phi$  states discussed above has significant contribution to their total decay widths. Thus, measuring the cross section of  $e^+e^- \rightarrow K_2^*(1430)K\pi$  with energy of collision up to 3 GeV will be a promising approach to identify these highly excited  $\phi$  states. As shown

in Fig. 3 (c), indeed there are many obvious enhancement structures existing in collision energy range of 2.4~2.7 GeV for  $e^+e^- \rightarrow K_2^{*0}(1430)K^-\pi^+$ , which may correspond to these discussed  $\phi$  mesons. More precise data is expected in future experiment.

### III. SUMMARY

In the past decades, the process of  $e^+e^-$  annihilation into light mesons can be as ideal platform to probe light vector mesonic state. A typical example is the observation of  $Y(2175)$ , which had stimulated theorist's interest in revealing its inner structure [11–16]. In recent years, BESIII, as main force of studying light hadron spectroscopy, has accumulated more and more data of  $e^+e^-$  annihilation into light mesons [29, 52–58]. Especially, these experimental measurements from BESIII make that constructing light unflavor vector mesons around 2 GeV becomes possible [12, 49, 57, 58].

Although big progress has been made by both experimentalist and theorist, our knowledge of these light unflavor vector mesons existing in the mass range of 2.4 ~ 3 GeV is not abundant, which inspires our attention.

In this work, we carry out the investigation of the spectroscopy behavior of these light unflavor vector mesons existing in the mass range of 2.4 ~ 3 GeV, which contains the information of their masses and their two-body OZI allowed strong decay behaviors. These predictions can provide crucial hints when hunting for these predicted light unflavor vector mesons.

As emphasized in the recent white paper released by BESIII [45], the study around light hadron will still be one of tasks of the BESIII experiment in the next ten years. According to our study, we strongly suggest our experimental colleague to pay attention to 2.4 ~ 3 GeV energy range of collision, which has close relation to these predicted light unflavor vector meson states.

### Acknowledgments

LMW would like to thank Lanzhou Center for Theoretical Physics to support his stay at Lanzhou University, where this work was finished. This work is supported by the China National Funds for Distinguished Young Scientists under Grant No. 11825503, National Key Research and Development Program of China under Contract No. 2020YFA0406400, the 111 Project under Grant No. B20063, the National Natural Science Foundation of China under Grant No. 12047501, and the projects funded by Science and Technology Department of Qinghai Province No. 2020-ZJ-728.

- 
- [1] M. Ablikim *et al.* [BES Collaboration], Observation of a resonance  $X(1835)$  in  $J/\psi \rightarrow \gamma\pi^+\pi^-\eta'$ , Phys. Rev. Lett. **95**, 262001 (2005).  
 [2] M. Ablikim *et al.* [BESIII Collaboration], Confirmation of

- the  $X(1835)$  and observation of the resonances  $X(2120)$  and  $X(2370)$  in  $J/\psi \rightarrow \gamma\pi^+\pi^-\eta'$ , Phys. Rev. Lett. **106**, 072002 (2011).  
 [3] M. Ablikim *et al.* [BESIII Collaboration], Observation of an

- anomalous line shape of the  $\eta'\pi^+\pi^-$  mass spectrum near the  $p\bar{p}$  mass threshold in  $J/\psi \rightarrow \gamma\eta'\pi^+\pi^-$ , Phys. Rev. Lett. **117**, no. 4, 042002 (2016).
- [4] M. Ablikim *et al.* [BES Collaboration], Observation of  $Y(2175)$  in  $J/\psi \rightarrow \eta\phi f_0(980)$ , Phys. Rev. Lett. **100**, 102003 (2008).
- [5] M. Ablikim *et al.* [BESIII Collaboration], Study of  $J/\psi \rightarrow \eta\phi\pi^+\pi^-$  at BESIII, Phys. Rev. D **91**, no. 5, 052017 (2015).
- [6] J. P. Lees *et al.* [BaBar Collaboration], Cross Sections for the Reactions  $e^+e^- \rightarrow K^+K^-\pi^+\pi^-$ ,  $K^+K^-\pi^0\pi^0$ , and  $K^+K^-K^+K^-$  Measured Using Initial-State Radiation Events, Phys. Rev. D **86**, 012008 (2012).
- [7] B. Aubert *et al.* [BaBar Collaboration], Measurements of  $e^+e^- \rightarrow K^+K^-\eta$ ,  $K^+K^-\pi^0$  and  $K_S^0K^\pm\pi^\mp$  cross-sections using initial state radiation events, Phys. Rev. D **77**, 092002 (2008).
- [8] C. P. Shen *et al.* [Belle Collaboration], Observation of the  $\phi(1680)$  and the  $Y(2175)$  in  $e^+e^- \rightarrow \phi\pi^+\pi^-$ , Phys. Rev. D **80**, 031101 (2009).
- [9] B. Aubert *et al.* [BaBar Collaboration], The  $e^+e^- \rightarrow K^+K^-\pi^+\pi^-$ ,  $K^+K^-\pi^0\pi^0$  and  $K^+K^-K^+K^-$  cross-sections measured with initial-state radiation, Phys. Rev. D **76**, 012008 (2007).
- [10] B. Aubert *et al.* [BaBar Collaboration], A Structure at 2175-MeV in  $e^+e^- \rightarrow \phi f_0(980)$  Observed via Initial-State Radiation, Phys. Rev. D **74**, 091103 (2006).
- [11] G. J. Ding and M. L. Yan,  $Y(2175)$ : Distinguish Hybrid State from Higher Quarkonium, Phys. Lett. B **657**, 49 (2007).
- [12] J. Z. Wang, L. M. Wang, X. Liu and T. Matsuki, Deciphering the light vector meson contribution to the cross sections of  $e^+e^-$  annihilations into the open-strange channels through a combined analysis, [arXiv:2106.14582 [hep-ph]].
- [13] Z. G. Wang, Analysis of the  $Y(2175)$  as a tetraquark state with QCD sum rules, Nucl. Phys. A **791**, 106 (2007).
- [14] A. Martinez Torres, K. P. Khemchandani, L. S. Geng, M. Napsuciale and E. Oset, The  $X(2175)$  as a resonant state of the  $\phi K\bar{K}$  system, Phys. Rev. D **78**, 074031 (2008).
- [15] H. X. Chen, X. Liu, A. Hosaka and S. L. Zhu, The  $Y(2175)$  State in the QCD Sum Rule, Phys. Rev. D **78**, 034012 (2008).
- [16] E. Klempt and A. Zaitsev, Glueballs, Hybrids, Multiquarks. Experimental facts versus QCD inspired concepts, Phys. Rept. **454**, 1 (2007).
- [17] X. Wang, Z. F. Sun, D. Y. Chen, X. Liu and T. Matsuki, Non-strange partner of strangeonium-like state  $Y(2175)$ , Phys. Rev. D **85**, 074024 (2012).
- [18] T. Barnes, N. Black and P. R. Page, Strong decays of strange quarkonia, Phys. Rev. D **68**, 054014 (2003).
- [19] A. Antonelli *et al.* [FENICE Collaboration], Measurement of the total  $e^+e^- \rightarrow \text{hadrons}$  cross-section near the  $e^+e^- \rightarrow N\bar{N}$  threshold, Phys. Lett. B **365**, 427 (1996).
- [20] A. B. Clegg and A. Donnachie,  $\rho$ 's in 6  $\pi$  States From Materialization of Photons, Z. Phys. C **45**, 677 (1990).
- [21] A. Hasan and D. V. Bugg, Amplitudes for  $p\bar{p} \rightarrow \pi\pi$  from 0.36-GeV/c to 2.5-GeV/c, Phys. Lett. B **334**, 215 (1994).
- [22] D. V. Bugg, Four sorts of meson, Phys. Rept. **397**, 257 (2004).
- [23] M. Atkinson *et al.* [Omega Photon Collaboration], Evidence for a  $\omega\rho^\pm\pi^\mp$  State in Diffractive Photoproduction, Z. Phys. C **29**, 333 (1985).
- [24] S. U. Chung *et al.*, Exotic and  $q\bar{q}$  resonances in the  $\pi^+\pi^-\pi^-$  system produced in  $\pi^-p$  collisions at 18-GeV/c, Phys. Rev. D **65**, 072001 (2002).
- [25] A. V. Anisovich *et al.*,  $I = 0, C = -1$  mesons from 1940 to 2410 MeV, Phys. Lett. B **542**, 19 (2002).
- [26] D. V. Bugg, Partial wave analysis of  $\bar{p}p \rightarrow \bar{\Lambda}\Lambda$ , Eur. Phys. J. C **36**, 161 (2004).
- [27] M. Atkinson *et al.* [Omega Photon Collaboration], photon diffractive dissociation to  $\rho\rho\pi$  and  $\rho\pi\pi$  states, Z. Phys. C **38**, 535 (1988).
- [28] B. Aubert *et al.* [BaBar], The  $e^+e^- \rightarrow 3(\pi^+\pi^-), 2(\pi^+\pi^-\pi^0)$  and  $K^+K^-2(\pi^+\pi^-)$  cross sections at center-of-mass energies from production threshold to 4.5-GeV measured with initial-state radiation, Phys. Rev. D **73**, 052003 (2006).
- [29] M. Ablikim *et al.* [BESIII], Measurement of the  $e^+e^- \rightarrow \pi^+\pi^-\pi^0$  Cross Section from 0.7 GeV to 3.0 GeV via Initial-State Radiation, [arXiv:1912.11208 [hep-ex]].
- [30] J. P. Lees *et al.* [BaBar], Cross Sections for the Reactions  $e^+e^- \rightarrow K^+K^-\pi^+\pi^-$ ,  $K^+K^-\pi^0\pi^0$ ,  $K^+K^-K^+K^-$  Measured Using Initial-State Radiation Events, Phys. Rev. D **86**, 012008 (2012).
- [31] C. P. Shen *et al.* [Belle], Observation of the  $\phi(1680)$  and the  $Y(2175)$  in  $e^+e^- \rightarrow \phi\pi^+\pi^-$ , Phys. Rev. D **80**, 031101 (2009).
- [32] Q. T. Song, D. Y. Chen, X. Liu and T. Matsuki, Charmed-strange mesons revisited: mass spectra and strong decays, Phys. Rev. D **91**, 054031 (2015).
- [33] A. V. Anisovich, V. V. Anisovich, V. N. Markov, M. A. Matveev, V. A. Nikonov and A. V. Sarantsev, Radiative decays of quarkonium states, momentum operator expansion and nilpotent operators, J. Phys. G **31**, 1537 (2005).
- [34] W. Roberts and B. Silvestre-Brac, General method of calculation of any hadronic decay in the  $p$  wave triplet model, Acta Phys. Austriaca **11**, 171 (1992).
- [35] H. G. Blundell, Meson properties in the quark model: A look at some outstanding problems, 1996.
- [36] L. M. Wang, Q. S. Zhou, C. Q. Pang and X. Liu, Potential higher radial excitations in the light pseudoscalar meson family, Phys. Rev. D **102**, no.11, 114034 (2020).
- [37] J. S. Yu, Z. F. Sun, X. Liu and Q. Zhao, Categorizing resonances  $X(1835)$ ,  $X(2120)$  and  $X(2370)$  in the pseudoscalar meson family, Phys. Rev. D **83**, 114007 (2011).
- [38] L. P. He, X. Wang and X. Liu, Towards two-body strong decay behavior of higher  $\rho$  and  $\rho_3$  mesons, Phys. Rev. D **88**, no. 3, 034008 (2013).
- [39] Z. C. Ye, X. Wang, X. Liu and Q. Zhao, The mass spectrum and strong decays of isoscalar tensor mesons, Phys. Rev. D **86**, 054025 (2012).
- [40] B. Wang, C. Q. Pang, X. Liu and T. Matsuki, Pseudotensor meson family, Phys. Rev. D **91**, no. 1, 014025 (2015).
- [41] K. Chen, C. Q. Pang, X. Liu and T. Matsuki, Light axial vector mesons, Phys. Rev. D **91**, no. 7, 074025 (2015).
- [42] D. Guo, C. Q. Pang, Z. W. Liu and X. Liu, Study of unflavored light mesons with  $J^{PC} = 2^{--}$ , Phys. Rev. D **99**, no. 5, 056001 (2019).
- [43] C. Q. Pang, J. Z. Wang, X. Liu and T. Matsuki, A systematic study of mass spectra and strong decay of strange mesons, Eur. Phys. J. C **77**, no. 12, 861 (2017).
- [44] C. Q. Pang, Y. R. Wang and C. H. Wang, Prediction for  $5^{++}$  mesons, Phys. Rev. D **99**, no. 1, 014022 (2019).
- [45] M. Ablikim *et al.* [BESIII], Future Physics Programme of BESIII, Chin. Phys. C **44**, no.4, 040001 (2020).
- [46] S. Godfrey and N. Isgur, Mesons in a Relativized Quark Model with Chromodynamics, Phys. Rev. D **32**, 189 (1985).
- [47] P. A. Zyla *et al.* [Particle Data Group], Review of Particle Physics, PTEP **2020**, no.8, 083C01 (2020).
- [48] A. V. Anisovich, C. A. Baker, C. J. Batty, D. V. Bugg, L. Montanet, V. A. Nikonov, A. V. Sarantsev, V. V. Sarantsev and B. S. Zou, Combined analysis of meson channels with  $I = 1$ ,  $C = -1$  from 1940 to 2410 MeV, Phys. Lett. B **542**, 8-18 (2002).
- [49] L. M. Wang, J. Z. Wang and X. Liu, Toward  $e^+e^- \rightarrow \pi^+\pi^-$  annihilation inspired by higher  $\rho$  mesonic states around 2.2 GeV, Phys. Rev. D **102**, no.3, 034037 (2020).



- [50] M. Jacob and G. C. Wick, On the General Theory of Collisions for Particles with Spin, *Annals Phys.* **7**, 404-428 (1959)
- [51] C. Q. Pang, Excited states of  $\phi$  meson, *Phys. Rev. D* **99**, no.7, 074015 (2019).
- [52] M. Ablikim *et al.* [BESIII], Study of the process  $e^+e^- \rightarrow \phi\eta$  at center-of-mass energies between 2.00 and 3.08 GeV, *Phys. Rev. D* **104**, no.3, 032007 (2021).
- [53] M. Ablikim *et al.* [BESIII], Cross section measurement of  $e^+e^- \rightarrow K_S^0 K_L^0$  at  $\sqrt{s} = 2.00 - 3.08$  GeV, [arXiv:2105.13597 [hep-ex]].
- [54] M. Ablikim *et al.* [BESIII], Cross section measurements of  $e^+e^- \rightarrow K^+K^-K^+K^-$  and  $\phi K^+K^-$  at center-of-mass energies from 2.10 to 3.08 GeV, *Phys. Rev. D* **100**, no.3, 032009 (2019).
- [55] M. Ablikim *et al.* [BESIII], Observation of a structure in  $e^+e^- \rightarrow \phi\eta'$  at  $\sqrt{s}$  from 2.05 to 3.08 GeV, *Phys. Rev. D* **102**, no.1, 012008 (2020).
- [56] M. Ablikim *et al.* [BESIII], Measurement of the Born cross sections for  $e^+e^- \rightarrow \eta'\pi^+\pi^-$  at center-of-mass energies between 2.00 and 3.08 GeV, *Phys. Rev. D* **103**, no.7, 072007 (2021).
- [57] M. Ablikim *et al.* [BESIII], Measurement of  $e^+e^- \rightarrow K^+K^-$  cross section at  $\sqrt{s} = 2.00 - 3.08$  GeV, *Phys. Rev. D* **99**, no.3, 032001 (2019).
- [58] M. Ablikim *et al.* [BESIII], Observation of a Resonant Structure in  $e^+e^- \rightarrow K^+K^-\pi^0\pi^0$ , *Phys. Rev. Lett.* **124**, no.11, 112001 (2020).